Journal of the Korean Physical Society, Vol. 32, No. 5, May 1998, pp. L635∼L638

Global Modeling of the Ion-Pumping Effect in a Helicon-Plasma Discharge

M. Yoon*, S. C. Kim, H. J. Lee and J. K. Lee

Department of Physics, Pohang University of Science and Technology, Pohang 790-784

(Received 20 January 1998, in final form 23 April 1998)

The ion-pumping effect in helicon discharges was investigated numerically with a time-dependent volume-averaged global model for the plasma density and the electron temperature. By adjusting the neutral gas density and the absorbed power, the ion-current density as a function of time was obtained. The ion-current density obtained with our method compares well with the experimental results.

A high-density helicon discharge is known as an efficient ion pump [1]. Its mechanism can be described as follows: When part of a neutral gas is ionized, the ions are accelerated by the pre-sheath electric field with the Bohm velocity. Thus, an ion reaches the wall at a much faster speed than the thermal speed of the neutral gas. When it hits the wall, the ion recombines to become a neutral, and this neutral either gets pumped out or slowly diffuses back toward the center at the thermal speed. Because the neutrals can reach the pump faster in the presence of a plasma, the neutral pressure in the discharge chamber, which is lower than without plasma, reaches a steady state during the rf pulse. Such phenomena have been observed experimentally and reported elsewhere [1,2]. Here, we investigate the ion-pumping effect with the help of a global model [3,4] for the plasma discharge. We will first describe the equations in our global model and the method of solving them. We then apply the model to simulate the ion-pumping effect.

The global model used in our analysis is a plasma-discharge model and solves the time-dependent equations of the volume-averaged zero-dimensional plasma variables. The model consists of a set of conservation equations for the particle-number density and the energy.

The variable mobility model [5] leads to a nonlinear diffusion equation for the plasma-density profile in the steady state. It is found that the density is relatively uniform within most of the discharge region and drops sharply near the walls.

In order to determine the approximate plasma densities at the sheath edges, Godyak solved the diffusion equation analytically [6] to obtain in cylindrical coordinates

$$h_L = \frac{n_{sL}}{n_e} \approx 0.86 \left(3 + \frac{L}{2\lambda_i}\right)^{-1/2} ,$$
$$h_R = \frac{n_{sR}}{n_e} \approx 0.80 \left(4 + \frac{R}{\lambda_i}\right)^{-1/2} , \quad (1)$$

where h_L and h_R are the plasma densities at the axial and the radial sheath edges normalized to the electron density and L and R are the lengths of the axial and the radial discharge regions, respectively. With these expressions, the balance of electron-ion pairs generated in the plasma and lost at the walls can be written as

$$\frac{\partial n_e}{\partial t} = \frac{dn_e}{dt} = K_{iz} n_e n_g - \frac{(h_L A_L + h_R A_R)}{V} n_e u_B , \quad (2)$$

where $V = \pi R^2 L$ is the plasma volume, n_g is the neutral gas density, and $A_L = 2\pi R^2$ and $A_R = 2\pi RL$ are the effective areas of the axial and the radial sheaths. The ion acoustic (or Bohm) velocity u_B is given by $(eT_e/M)^{1/2}$. The ionization rate constant K_{iz} is a function of T_e alone and can be written in the fitted form of

$$K_{iz} = c_{1,iz} \exp\left(-\frac{c_{2,iz}}{T_e}\right) . \quad (3)$$

For argon gas, the rate constants are given by Stewart *et al.* [6] as $c_{1,iz} = 1.235 \times 10^{-7}$ cm^3/s and $c_{2,iz}$=18.69 eV. Note that in Eq. (2), we have changed the partial derivative to a total derivative because in the global model, the electron density is independent of the position.

Taking into account the secondary electron emission and radiative recombination, Eq. (2) can be expressed in a more general form [3]:

$$\frac{dn_e}{dt} = K_{iz} n_e n_g - \frac{\Gamma_e}{d_{eff}} + \gamma_s \frac{\Gamma_i}{d_{eff}} - \alpha n_i n_e , \quad (4)$$

*E-mail: moohyun@postech.ac.kr

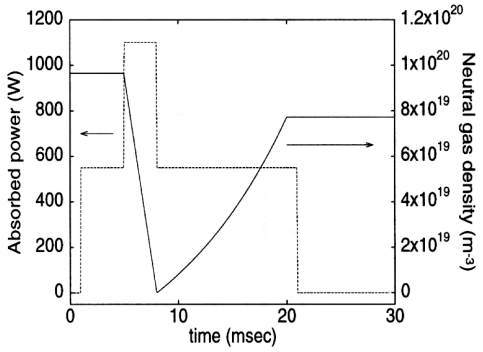

Fig. 1. The variation of the absorbed rf power (dotted line) and the neutral gas density(solid line) adopted in the global model. The high-current phase of the helicon discharge was assumed to begin at $t = 5$ msec and to end at $t = 8$ msec, during which the neutral gas was assumed to be depleted linearly to zero and then to slowly diffuse back to the discharge region.

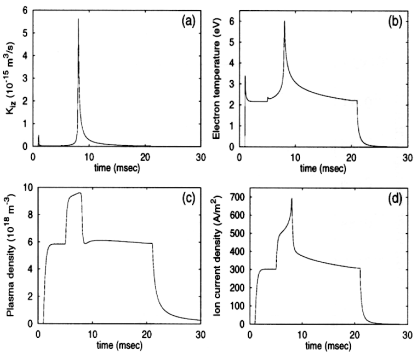

Fig. 2. (a) Variation of the ionization rate constant K_{iz} as a function of time. (b) Variation of the electron temperature as a function of time. (c) Variation of the plasma density as a function of time. (d) Variation of the ion current density as a function of time.

where n_i is the ion density, which we take to be $n_i \approx n_e$, and γ_s is the secondary electron-emission coefficient, which depends on the material property of the surface. The radiative recombination coefficient α between electrons and ions is 2×10^{-16} m^3/s at 3100 K for argon [7]. The term due to recombination loss is found to be comparable to the one due to the wall loss, which varies between 10^{18} and 10^{22} m$^{-3}\cdot$ sec^{-1}. In the above equation, the effective plasma size d_{eff} is given by

$$d_{eff} = \frac{V}{h_L A_L + h_R A_R} = \frac{1}{2}\frac{RL}{Rh_L + Lh_R} \ . \tag{5}$$

We assume that the plasma is electrically neutral and the diffusion is ambipolar. This means that the electron and the ion fluxes toward the walls balance at all times. With this assumption, the electron and the ion fluxes leaving the plasma are

$$\Gamma_e = \Gamma_i = n_s u_B \ , \tag{6}$$

where n_s is the density at the sheath edge.

The power balance equation is given by [3]

$$\frac{d}{dt}\Big(\frac{3}{2}n_e k T_e\Big) = \frac{P_{abs}}{V} - \frac{P_c}{V} - \frac{\Gamma_i}{d_{eff}}\Big[(1-\gamma_s)e|V_s| + \frac{kT_e}{2}\Big] - \frac{\Gamma_e}{d_{eff}} 2kT_e - \alpha\frac{3}{2}kT_e n_i n_e \ , \tag{7}$$

where P_{abs} is the total power absorbed, which is assumed to be known, V_s is the sheath potential, and P_c/V is the rate of collisional energy loss per unit volume given by

$$\frac{P_c}{V} = n_e n_g K_{iz}\varepsilon_c = n_e n_g (K_{iz}\varepsilon_{iz} + K_{ex}\varepsilon_{ex} + K_{el}\varepsilon_{el}) \tag{8}$$

with K_{iz}, K_{ex}, and K_{el} being the rate constants (in m^3/s), and $\varepsilon_{iz}, \varepsilon_{ex}$, and ε_{el} (in eV) the energies lost per ionizational, excitational, and elastic collisions, respectively. These values can be found elsewhere [6]. The energy lost due to elastic (polarization) scattering is given by $\varepsilon_{el} = 3m_e kT_e/M$, where m_e is the mass of the electron.

In Eq. (7), the third term on the right-hand side is the sum of the power lost by the ion flux to the wall and the power gain due to the secondary electrons emitted from the wall due to ion bombardment. The potential difference V_s between the wall and the bulk plasma, which has a negative value, can be approximately obtained based on the assumption of ambipolar diffusion, $\Gamma_i = \Gamma_e$, and a collisionless sheath with the secondary emission effect. For argon gas, it is given by [4]

$$eV_s = -[4.7 - \ln(1+\gamma_s)]kT_e \ . \tag{9}$$

The fourth term in Eq. (7) is the power loss due to the escaping electrons, which have a Maxwellian distribution. The last term is the power loss due to the recombination of electrons and ions. Equations (4) and (7) can be solved simultaneously to obtain n_e and T_e as functions of time. The chosen initial conditions are $n_{e_0} = 10^{17}$ m^{-3} and $T_{e_0} = 0.001$ eV.

If we apply the above equations to the typical case [2] of a Helicon discharge, $p = 3$ mTorr, $P_{abs} = 1100$ W, $R = 5$ cm, and $L = 70$ cm, we obtain $\lambda_i \approx 1.04$ cm, $d_{eff} \approx 2.47$ m, and $n_g d_{eff} \approx 2.38 \times 10^{20}$ m^{-2}. These parameters give $T_e \approx 2.2$ eV. In calculating d_{eff}, we have neglected the loss in the radial direction (*i.e.*, $h_R = 0.$) because of the confinement due to the magnetic field, and we have taken into account the loss in the axial direction only (*i.e.*, $h_L \approx 0.1418$). At $T_e \approx 2.2$ eV, we have $\varepsilon_c \approx 80$ eV and $\varepsilon_T \approx 95.8$ eV, where ε_c and ε_T are the energy lost per each collision by one electron and the total energy lost by one electron including wall loss, respectively. These parameters give $n_e \approx 1.4 \times 10^{19}$ m^{-3} in the steady state.

The actual experimental apparatus of Ref. 2 consists of two chambers; one is a discharge chamber of 5 cm by 70 cm and the other is a reaction chamber of 15 cm by 40 cm. In our model, we have taken into account the discharge chamber only, neglecting the diffusion to the reaction chamber because the present global model can not deal with two chambers properly. This requires further improvement which will be the subject of future work on our global model.

In the modeling of the ion-pumping effect described in the beginning, we used the above parameters which were those used in the experiment performed at Korean Advanced Institute of Science and Technology (KAIST) [2]. For the simulation, we assumed that in the low-current phase of the helicon discharge, 50% of the rf power was absorbed while in the high-current phase, the full 1100 W rf power was absorbed. In accordance with the experiment, the rf power was turned on for 20 msec and turned off afterwards. To supply the particle losses corresponding to 1100 W of absorbed power and 200 eV for each ionization [1], 3.5×10^{19} neutral atoms must be ionized per second. Because a discharge tube of 5 cm in radius and 70 cm in length contains 6×10^{17} neutrals at 3 mTorr, the neutrals will be depleted in about a few tenth of a millisecond. However, this is based on only a crude approximation. In view of the experimental result [2] in the high-current phase of the discharge, the depletion of the neutral gas was assumed to occur for 3 msec, and during this period, the neutral gas was assumed to decrease linearly according to

$$n_g(t) = n_{g0}\Big(1 - \frac{t - t_1}{t_2 - t_1}\Big) \ . \tag{10}$$

Thus, at $t = t_1$, the neutral gas starts depleting, and at $t = t_2$, it is completely depleted in the central region of the discharge tube.

The diffusion of the neutral gas to the center of the discharge region by recombination of ions and electrons near the wall and the new inflow of gas from an external source are difficult to incorporate in the model. Here, we assumed that after the complete depletion, the neutral gas at the center increased exponentially according to

$$n_g(t) = f n_{g0} \frac{e^{\gamma(t-t_2)/(t_3-t_2)} - 1}{e^{\gamma} - 1} \ , \tag{11}$$

where γ is the rate of increase of the neutral gas, which we take to be 1, and t_3 is the time when $n_g(t_3) = f n_{g0}$, where f is the fraction of the initial neutral gas.

The γ_s in Eqs. (4) and (7) has the effect of increasing the plasma density and the electron temperature to some extent. However, because of its smallness, we ignored it in our calculation. Inclusion of γ_s would not significantly modify our result.

Figure 1 shows the absorbed rf power and the variation of the neutral gas adopted in our model. The rf power was turned on at $t = 1$ msec, and the low-current phase (*i.e.*, 50% efficiency) was assumed to be launched. The high-current phase was then started at $t = 5$ msec and continued until $t = 8$ msec. At $t = 8$ msec, the discharge was assumed to return to the low-current phase because at that time, the neutral gas was completely depleted. The low-current phase continued until $t = 21$ msec when the rf was completely turned off. The depletion and the inflow of the neutral gas are also depicted in Fig. 1 with a solid line. We assumed that after the complete depletion at $t = 8$ msec, the neutral gas slowly returned to about 80% (*i.e.*, $f = 0.8$) of the original density n_{g0} because our calculation revealed that about 20% of the initial gas remained in the discharge region as a plasma. However, when $f = 1.0$, the result did not change significantly.

Figure 2(a) shows the ionization rate constant K_{iz} as a function of time. It is seen that the K_{iz} increases rapidly and peaks at $t = 8$ msec when the electron temperature T_e is greatest. Because of its dependence on T_e (see Eq. (3)), the behavior of K_{iz} can be understood with the help of Fig. 2(b), which shows the electron temperature (eV) as a function of time on the same horizontal scale as used in Figs. 1 and 2(a). After the onset of the high-current phase at $t = 5$ msec, the electron temperature increases sharply because of the small collisional energy loss, as Eq. (7) shows. After the peak at $t = 8$ msec, the electron temperature starts decreasing to reach a new equilibrium. The initial peak at $t = 1$ msec and the small bump in T_e at around $t = 5$ msec is due to the sudden increase in the absorbed power at that time, which can be understood with the help of Eqs. (4) and (7). Immediately after the rf pulse has been turned on, all the loss terms in Eqs. (4) and (7) are so small that they can be neglected to a good approximation. For example, immediately after 1 msec, we have approximately 10^5 W/m^3 for the first term, 10^4 W/m^3 for the second term, 10^3 W/m^3 for the third plus fourth terms, and 10^2 W/m^3 for the last term on the right-hand side of Eq. (7). We, thus, have

$$\frac{1}{T_e}\frac{dT_e}{dt} \approx \frac{2P_{abs}}{3n_e k T_e V} - \Big(\frac{2\varepsilon_c}{3T_e} + 1\Big) K_{iz} n_g \ . \tag{12}$$

Because of small T_e at the initial stage, K_{iz} is also small, as Fig. 2(a) shows, so that the second term on the right-hand side can be neglected. Therefore, T_e rises sharply at a rate given by the first term on the right. The peak value depends on the initial electron density. This explains the first peak around $t = 1$ msec in Fig. 2(b). Once T_e reaches a peak, it starts decaying to reach the steady-state temperature, as shown in Fig. 2(b), during $t = 2-5$ msec. In the high-current phase (*i.e.*, high absorbed rf power), the neutral gas also decays because of the high ionization rate. Inserting Eq. (10) into Eq. (12) and using $\varepsilon_c/T_e \approx 40 \gg 1$, we see that the sign of dT_e/dt must change before $t = t_2 = 8$ msec; therefore, T_e rises again to a peak value at $t = 8$ msec. As n_g increases again in the low-current phase ($t > 8$ msec), T_e now slowly decays to a steady-state value, as shown in Fig. 2(b). In the figure, the steady-state electron temperature is seen to be 2.2 eV, which agrees with our estimate above.

Figure 2(c) describes the plasma density as a function of time, again with the same horizontal time scale. At

the beginning of the high-current phase at $t = 5$ msec, because of the small loss, we can neglect the last three terms on the right-hand side of Eq. (4) to yield

$$\frac{1}{n_e}\frac{dn_e}{dt} = K_{iz} n_g \ . \tag{13}$$

Therefore, as the high-current phase is launched, the plasma density rises rapidly at a rate given by $K_{iz} n_g$. The rate of increase then decreases as n_g falls, which may explain the decrease of the slope in the high-current phase in Fig. 2(c). At the end of the high-current phase at $t = 8$ msec, the plasma density falls sharply because of the complete depletion of the neutral gas. The steady-state value of n_e is shown to be 6×10^{18} m^{-3} in Fig. 2(c), which agrees with our estimate above (*i.e.*, at $P = 550$ W, $n_e \approx 7 \times 10^{18}$ m^{-3}).

Finally, Fig. 2(d) shows the evolution of the ion-current density J_i, which is to be compared with the experimental observations [1,2]. The ion-current density in this figure was calculated from $J_i = e n_e u_B h_L$; therefore, it is proportional to $T_e^{1/2}$ and n_e. The change in the slope of J_i during $t = 5 - 8$ msec in the figure is due to a change in the slope of n_e, as Fig. 2(c) indicates. Such a change in slope has not been reported in experiments [1,2]. Nevertheless, the general behavior of J_i is similar to the experimental results, especially to Fig. 35 of Ref. 1. The decay pattern from 8 msec to 21 msec in Fig. 2(d) is also similar to the one observed in a recent experiment [8] on plasma-source ion implantation. It should also be noted that the general behavior of the ion-current density in the ion-pumping effect can be predicted when assumptions about both the neutral gas depletion and the power absorption are made.

In conclusion, we have modeled the ion-pumping effect in a helicon discharge with a time-dependent global model. The global model, with appropriate assumptions for the neutral gas depletion and the power absorption, can simulate the ion-pumping effect reasonably well. The results shown in this report compare favorably with experimental results.

ACKNOWLEDGMENTS

This work was supported by the Basic Science Research Institute Program of the Ministry of Education, 1997, Project No. BSRI-97-2439 and the POSTECH/BSRI Special Fund.

REFERENCES

[1] F. F. Chen, *High Density Plasma Sources*, edited by O. A. Popov (Noyes Pub., Park Ridge, NJ, 1995), p. 52; R. W. Boswell, Plasma Phys. Controlled Fusion **26**, 1147 (1984).

[2] J-H. Kim and H-Y. Chang, Phys. Plasmas **3**, 1462 (1996).

[3] H. J. Lee and J. K. Lee, Jpn. J. Appl. Phys. **35**, 6252 (1996); T. H. Chung, S. H. Lee and J. K. Lee, J. Korean Phys. Soc. **10**, 40 (1997); N. S. Yoon, S. S. Kim, C. S. Chang and D. I. Choi, J. Korean Phys. Soc. **28**, 172 (1995); S. S. Kim, C. S. Chang and N. S. Yoon, J. Korean Phys. Soc. **29**, 678 (1996)

[4] M. A. Lieberman and A. J. Lichtenberg, *Principles of Plasma Discharge and Materials Processing* (Wiley, New York, 1994), Chaps. 5 and 10; M. A. Lieberman and S. Ashida, Memorandum No. UCB/ERL M95/83 (1995).

[5] V. A. Godyak, *Soviet Radio Frequency Discharge Research* (Delphic Associates, Falls Church, 1986).

[6] R. A. Stewart, P. Vitello and D. B. Graves, Plasma Sources Sci. Tech. **4**, 36 (1995); J. K. Lee, L. Meng, Y. K. Shin, H. J. Lee and T. H. Chung, Jpn. J. Appl. Phys. **36**, 5714 (1997).

[7] S. C. Brown, *Basic Data of Plasma Physics* (AIP Press, New York, 1994).

[8] Y. W. Choi, private communication.